Suppression of spin relaxation of conduction electrons by cyclotron motion

Z. Wilamowski*
Institute of Physics PAS, Al. Lotników 32/46, 02-668 Warsaw, Poland

W. Jantsch
Institut für Halbleiterphysik, Johannes Kepler Universität, A-4040 Linz, Austria

(Received 16 August 2003; revised manuscript received 23 October 2003; published 28 January 2004)

We investigate the spin relaxation of two-dimensional (2D) electrons in a Si/SiGe quantum well by means of electron spin resonance. Simultaneous observation of cyclotron resonance allows us to evaluate the influence of momentum scattering on spin relaxation. We identify thus a dominant contribution due to the D'yakonov-Perel mechanism which is expected to be more efficient for slow momentum-relaxation. The observed relaxation times of microseconds can be explained, however, only by an additional motional narrowing due to modulation of the spin-orbit coupling caused by the cyclotron motion. The latter is evidenced by the observed dependence of spin relaxation on the direction of applied magnetic field which changes the cyclotron frequency of the 2D electrons.

DOI: 10.1103/PhysRevB.69.035328 PACS number(s): 71.55.Eq, 76.30.Fc, 75.50.Pp, 75.30.Gw

I. INTRODUCTION

Spin-orbit (SO) coupling in semiconductor structures is crucial for many physical properties. Generally, the SO interaction governs the coupling between electronic and spin degrees of freedom.[1] On the one hand, SO coupling may allow electric manipulation or control of magnetic properties. On the other hand, it causes spin-dependent electronic properties which may allow one to read out a spin state by means of electrical features. Simultaneously, however, the presence of SO causes electron motion to affect the spin states, leading to spin relaxation and shortening of the spin memory.[2,3] Therefore, the SO interaction became a subject of intense interest again in the context of spintronics.

For applications where a long spin memory is the main goal,[4,5] silicon appears to be the best semiconductor. Si is characterized by a very weak SO coupling and present Si technology provides probably the magnetically purest material available: the concentration of paramagnetic impurities is extremely small and there is only one isotope of silicon, ^{29}Si, which has nuclear spin (1/2) at a natural abundance of less than 5%. Recently we found spin coherence times of the order of microseconds for Si quantum wells.[6,7] For spintronic applications the spin coherence should be as long as possible and therefore it is obviously necessary to investigate the mechanisms that limit the spin lifetime.

Among the different spin relaxation mechanisms two are of importance for pure material at low temperature ($T < 40$ K). Both are ruled by the momentum relaxation—i.e., the electron mobility—and by SO coupling. The first one is the Elliott-Yafet (EY) mechanism.[1,2] The EY treatment is based on the fact that due to the SO interaction spin is not a good quantum number and free carrier wave functions are of **k**-dependent mixed spin character. Therefore a scattering event changes also the spin state with some probability.

The second group of mechanisms, treated by D'yakonov and Perel, appears in systems lacking inversion or mirror symmetry.[3] In such a system, the SO interaction causes terms in the Hamiltonian containing products of odd powers of the **k** vector of the electron and spin. For higher symmetry these terms vanish. The low symmetry may be caused by the crystal structure[8]—then these effects are designated as ''bulk-inversion asymmetry'' (BIA) or by structure—e.g., by thin layers and surface states which cause an electric field in the layer.[9] Effects caused by the latter are attributed to ''structure-induced asymmetry'' (SIA). The SIA and BIA terms in the Hamiltonian cause spin splitting and thus they may be described by an effective, **k**-dependent magnetic field. They modify the spin precession frequency, causing a change of g factor and broadening of the spin resonance line.[6] Moreover, this field changes as the **k** vector of the electron, **k**, changes and thus they may cause spin relaxation.[7]

For a two-dimensional (2D) electron gas in a quantum well, which does not have mirror symmetry, two types of such effective fields may occur: namely, Bychkov-Rashba[9] (BR) and Dresselhaus[10,11] (DR) fields. Both types of fields are oriented within the 2D plane. The strength of the BR field is proportional to the electron momentum and it is independent of the direction of electron motion while the DR field strongly varies its strength with the direction of electron motion. Consequently, when the in-plane direction of the **k** vector, φ_k, is changed the BR field varies with φ_k while the cubic DR term has also a component changing with $3\varphi_k$.

In a previous paper[6] we analyzed the effect of the BR field on the g factor and the resonance linewidth for in-plane orientation of the magnetic field. In this paper we investigate the influence of momentum scattering and of cyclotron motion on the transverse and longitudinal spin relaxation rates. We find that the cyclotron motion, leading to additional modulation of the spin-orbit interaction, causes motional narrowing and, consequently, a reduction of the spin relaxation rates. A characteristic anisotropy of spin relaxation occurs since the cyclotron frequency of 2D carriers depends on the direction of the applied field. Finally, we discuss possible contributions of the BR and DR fields. Because the cubic DR field varies 3 time faster with φ_k as compared to the BR term, under the cyclotron motion the DR field should be

modulated faster, allowing us to distinguish both contributions to the spin relaxation.

II. EXPERIMENTAL DETAILS

A. Samples

Samples were grown by molecular beam epitaxy on 1000 Ω cm Si(001) substrates, which show complete carrier freeze-out below 40 K. A 20-nm-thick Si channel with tensile in-plane strain was deposited on a strain-relaxed buffer layer, which consists of a 0.5-μm-thick $Si_{0.75}Ge_{0.25}$ layer on top of a 2-μm-thick $Si_{1-x}Ge_x$ layer with compositional grading. The upper $Si_{0.75}Ge_{0.25}$ barrier was modulation doped with a 12.5-nm-thick, nominally undoped spacer layer and capped with 5 nm of Si. Three modulation-doped Si/SiGe structures with different donor concentrations were examined. The electron concentration could be changed persistently by illumination with band-gap light for different periods of time. Altogether the sheet electron concentration in the investigated samples could be varied in the range of 3×10^9–7×10^{11} cm^{-2}.

B. Spectrometer

All measurements were performed with a standard *X*-band ESR spectrometer at a microwave frequency of $\omega_0/2\pi = 9.4$ GHz. The sample is placed in the center of the rectangular TE_{102} cavity, at the maximum of the magnetic microwave field component $\mathbf{H}_1$, which is perpendicular to the applied static magnetic field $\mathbf{H}$, and at the minimum (node) of the electric field component, which is parallel to $\mathbf{H}$.

Making use of the loaded cavity resonance curve we estimate an H_1, corresponding to full klystron power (200 mW), of 0.9 G. We found that this value weakly depends on the sample position in the microwave cavity. Therefore we took this reference value for all measurements. The fact that our results are in good agreement with the direct measurements of spin relaxation by means of spin-echo methods[7,12] for the same sample shows that we estimate H_1 correctly.

In this apparatus, the sample can be rotated around an axis parallel to $\mathbf{H}_1$. The corresponding angle θ_H is defined to be zero when $\mathbf{H}$ is perpendicular to the sample layer (parallel to the growth direction) while $\theta = 90°$ stands for in-plane orientation.

C. Cyclotron resonance

The spectra are characterized by a strong broad line caused by the cyclotron resonance (CR), corresponding to the light electron mass ($m^* = 0.2m_0$) and a very narrow electron spin resonance (ESR) line due to spin resonance of the 2D electron gas corresponding to a *g* factor[6,7] very close to 2.

Analysis of the CR spectra in terms of the Drude model allows us to evaluate the momentum relaxation rate τ_k^{-1}. The latter depends on the doping concentration and varies strongly with carrier concentration, from 5×10^{10} s^{-1}, for the highest mobility sample, up to 10^{12} s^{-1} close to the metal-to-insulator transition.[13] For low-mobility samples the CR shape is close to Lorentzian, but for very high mobility it is well described by the Gaussian shape function.

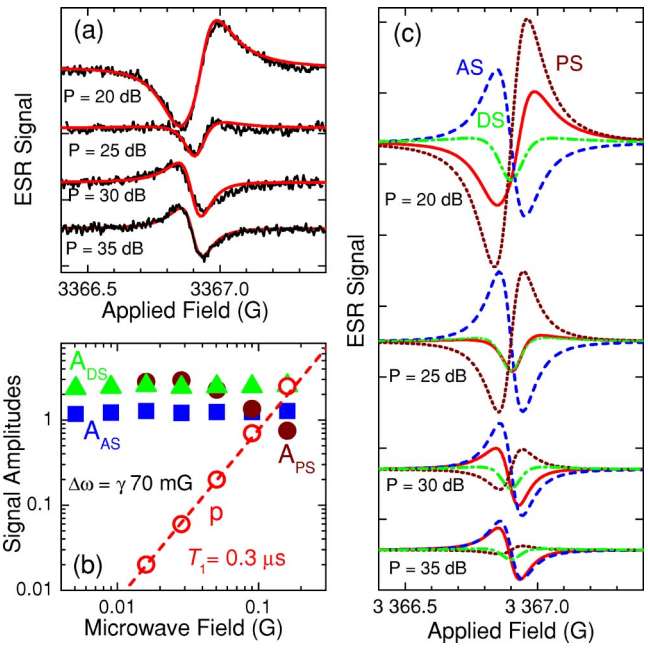

FIG. 1. ESR signal—i.e., the derivative of the microwave absorption as a function of magnetic field—for different microwave powers. Thick solid lines: fits according to Eq. (11) and shapes functions by Eqs. (1), (5), and (7). A common value of the resonance linewidths, $\Delta\omega/\gamma = 70$ mG, is found. Best fit values of the amplitudes A_{AS} (squares), A_{PS} (solid circles), and A_{DS} (triangles), fitted for individual spectra, are shown in (b). Open circles: reduced power *p* as defined by Eq. (3). The slope of *p* vs H_1 yields $T_1 = 0.3$ μs. In (c) deconvolution of the three components of the ESR signal with microwave power are shown. Dashed line: classical AS. Dotted line: PS. Dash-dotted line: DS.

D. Electron spin resonance signal

The spin resonance signal is very small as compared to that of the CR. The peak-to-peak amplitude of the derivative ESR is by 3 orders of magnitude smaller as compared to the CR signal. Since the ESR linewidth is by 4 orders of magnitude smaller, one can conclude that the integral CR absorption, before differentiation, is by 7 orders of magnitude bigger than the ESR absorption.

The observed ESR line shape is rather complex; it differs from the regular shape of an absorption line.[14] We relate this additional complexity to a strong electric absorption and to screening of the electric microwave field by high-mobility electrons. As is shown in Fig. 1, all spectra observed can be phenomenologically described by a sum of three types of signals: absorption signal (AS), dispersive signal (DS), and polarization signal (PS).

1. Absorption ESR signal

The AS is the signal related to the magnetic dipole transitions—the classical signal of spin resonance. In ESR of

conduction electrons it dominates at low microwave power only. The shape of the AS can be well fitted by the function

$$f'_{AS} = -\frac{1}{\pi}\frac{2h}{(1+p+h^2)^2}, \tag{1}$$

which is the field derivative of the handbook Lorentz shape function[15]

$$f_{AS} = \frac{1}{\pi}\frac{1}{1+p+h^2}. \tag{2}$$

Here we use normalized, dimensionless quantities: for the magnetic field H, we use $h=(H-H_0)/\Delta H$, where H_0 is the resonant field, $\Delta H = \Delta\omega/\gamma$ is the Lorentz linewidth, and γ is the gyroscopic factor, while the normalized microwave power

$$p = \gamma^2 H_1^2 T_1 / \Delta\omega \tag{3}$$

is proportional to the microwave power P—i.e., to the square of the amplitude of the magnetic component of the microwave, H_1, normalized by the resonance linewidth $\Delta\omega$ and the longitudinal spin relaxation rate $1/T_1$.

The linewidth at low microwave power, $\Delta\omega$, is given by the sum of the transverse spin relaxation rate, $1/T_2$, and half of the longitudinal spin relaxation rate, $1/2T_1$:

$$\Delta\omega = \frac{1}{2T_1} + \frac{1}{T_2}. \tag{4}$$

The amplitude of the AS is proportional to the square root of the microwave power, $P^{1/2}$. The absorption signal corresponds to the classical resonance absorption in our type of ESR experiment. The derivative of the AS is an odd function of the normalized field h.

2. Dispersion signal

The shape of the observed ESR lines of 2D conduction electrons in Si/SiGe is neither fully symmetric nor antisymmetric. It is similar to the so-called Dysonian line shape commonly observed in 3D metals where a small skin penetration depth causes the occurrence of the dispersion signal, in addition to the absorption signal. A 2D metallic layer differs from a 3D metal as the skin penetration depth is much larger than the thickness of the 2D layer. In that sense the microwaves can penetrate the 2D electron gas and the asymmetric signal observed cannot be related to the Dysonian effect. Nevertheless, the presence of the sample in the microwave cavity can strongly perturb the standing-wave mode in the cavity. If $\omega_0\tau_k \ll 1$, then the nonresonant electric absorption of the microwaves and the resulting decrease of the quality factor of the cavity are dominant. The AS is partially suppressed, but as long as the electric conductivity does not depend on the spin structure, the ESR line shape is not affected. On the other hand, for high-mobility electrons, when $\omega_0\tau_k \gg 1$, the imaginary part of the electric conductivity dominates; i.e., the electron motion is delayed in phase as compared to the microwave field. As a result, a DS of the ESR occurs.

The dispersion signal is well fitted by the dispersion component of the Lorentz shape function. The derivative is an even function of the normalized field h:

$$f'_{DS} = \frac{1}{\pi}\frac{1+p-h^2}{(1+p+h^2)^2}. \tag{5}$$

Our observation (see, e.g., data shown in Fig. 1) shows that when the signal is a sum of AS and DS then both signals are characterized by the same parameters $\Delta\omega$ and T_1. As a result an asymmetric, ''Dysonian'' line shape is observed. The ratio of the AS to DS amplitudes depends on the electron mobility and the direction of the applied magnetic field. The AS is dominant in high-mobility samples for low microwave power and in-plane orientation ($\theta_H = 90°$). The DS is proportional to $P^{1/2}$.

3. Electrically detected polarization signal

The observed spectra cannot be described by a combination of AS and DS alone. A phenomenological analysis of the spectra shows that there must be an additional contribution with the following properties.

(i) It has the shape of an odd-parity function, similar in shape to the AS [see Eq. (1)].

(ii) For high microwave power the linewidth of this signal is considerably bigger as compared to the widths of the AS and DS.

(iii) It has a different dependence of the signal amplitude on microwave power: at low power a proportionality to $P^{3/2}$ is well obeyed.

These properties bring us to the conclusion that this additional contribution results from a change of the electric absorption caused by a dependence of the electric conductivity (CR) on the polarization of the electron spin system. In fact, the electric absorption scales with the microwave electric field, $E_1 \propto P^{1/2}$. In addition, for small power the deviation of the spin polarization from its thermodynamic equilibrium, $\eta(h,p) - \eta_0$, is expected to be proportional to the spin resonance absorption—i.e., proportional to the absorption function, as described by Eq. (2), and to power P. Together, the two factors lead to the observed $P^{3/2}$ dependence. This explains also the similar line shapes of AS and PS.

To fit the experimental data we use the shape function

$$f_{PS} = \frac{2+p+2h^2}{2(1+p+h^2)^2} \tag{6}$$

and its field derivative

$$f'_{PS} = -\frac{2ph(1+h^2)}{(1+p+h^2)^3}. \tag{7}$$

They were obtained under the assumption that the electric conductivity σ is a quadratic function of the spin polariza-

tion, $\sigma(p,h)=\sigma_0(1+\delta_{PS}\eta^2(p,h)+\cdots)$, and the PS is proportional to the change of electric conductivity:

$$S_{PS}\propto P^{1/2}(\sigma(p,h)-\sigma_0)=P^{1/2}\delta_{PS}(\eta^2(p,h)-\eta_0^2), \quad (8)$$

due to a change of spin polarization caused by the ESR absorption. Here δ_{PS} is the material parameter describing the dependence of electric conductivity on spin polarization and the dependence of spin polarization on microwave power and the applied field was obtained from the balance of the absorbed and dissipated powers at steady-state conditions (slow passage):

$$\eta(p,h)=\eta_0\frac{1+h^2}{1+p+h^2}. \quad (9)$$

The change of the squares of the spin polarization is then proportional to the shape function as described by Eq. (6). The expression takes the form $\eta^2(p,h)-\eta_0^2=-2p\ \eta_0^2 f_{PS}(p,h)$.

Finally, the PS amplitude is described by the shape function (6):

$$S_{PS}\propto P^{1/2}p\,\eta_0^2 f_{PS}(p,h). \quad (10)$$

It scales with $P^{3/2}$ and the square of the equilibrium spin polarization η_0^2.

As is shown in Fig. 1(c) the shape of the PS for small microwave power ($p\ll 1$) tends to the Lorentzian shape, as described by Eqs. (1) and (2). For high power ($p\gg 1$), the derivative is still an odd function of h, similar to the Lorentzian shape function, but the peak-to-peak linewidth of the PS [Eq. (7)] is by a factor $3^{1/2}$ bigger as compared to the width of the AS [Eq. (2)].

AS and PS are of similar shapes. They can be distinguished experimentally by an analysis of power dependences. The AS increases with $P^{1/2}$ while the PS increases with $P^{3/2}$.

In the case of a negative amplitude of PS, as is shown in Fig. 1, at a certain intermediate power, the AS and PS compensate each other and the DS is only seen. At high power the PS dominates.

4. Deconvolution of three signal components

The analysis of an individual ESR spectrum does not allow one to deconvolute the spectrum or to determine the amplitude of the three contributing signals and thus to evaluate all important quantities. Deconvolution becomes possible only considering a set of spectra, measured for various microwave powers by simultaneous analysis. In that case we describe the spectra by the same formula

$$S'(p,h)=P^{1/2}(A_{AS}f'_{AS}+A_{DS}f'_{DS}+pA_{PS}f'_{PS}). \quad (11)$$

Here the shape functions are given by Eqs. (1), (5), and (7). The amplitudes of the contributing signals, A_{AS}, A_{DS}, and A_{PS}, the low-power linewidth $\Delta\omega$, and the longitudinal spin relaxation time T_1 are treated as five independent fitting parameters. We look for the best fit to the whole set of measured spectra.

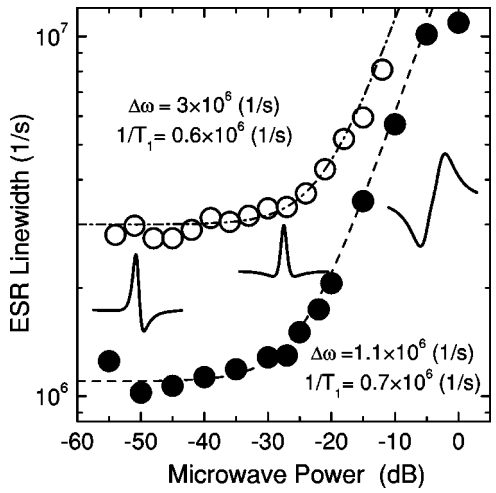

FIG. 2. Dependences of the ESR linewidth on microwave power for two different Si/SiGe samples (solid and open dots). At low power the linewidth stands for $\Delta\omega$. The line broadening caused by saturation of the ESR signals allows us to evaluate the longitudinal relaxation rate $1/T_1$. The icons show the evolution of the line shape for different powers.

These parameters are weakly correlated. Some of them can be evaluated directly without undergoing the whole procedure. In particular, the signal measured at low microwave power has a very small contribution of a PS. Moreover, in this limit the saturation effect can be also neglected. In that case only three parameters are of importance: namely, the amplitudes of the AS and the DS and the total linewidth. They can be easily evaluated from each spectrum independently—the linewidth can be measured directly, and the ratio A_{AS}/A_{DS} can be obtained from the asymmetry of the line or by a numerical separation of the even and odd contributions.

On the other hand, because the PS increases faster with increasing microwave power, the amplitude of the signal at high power directly yields A_{PS}.

Evaluation of T_1 needs more careful analysis. According to handbooks,[15] T_1 can be evaluated from the analysis of either the amplitude or linewidth. In the case of the discussed ESR signal, because of superposition of three signals, the analysis of the amplitude is possible when the shapes and amplitudes of all spectra, measured for different powers, are simultaneously fitted.

The evaluation of T_1 from the power dependence of the linewidth is much simpler. An example is shown in Fig. 2. In the low-power limit $p\ll 1$, the linewidth is equal to $\Delta\omega$, and in the high-power limit $p\gg 1$, the linewidth increases with H_1. For the AS, $\Delta\omega_p(p)\cong\Delta\omega^{1/2}\ \gamma\ H_1\ T_1^{1/2}$, and for PS the linewidth, $\Delta\omega_p(p)=3^{1/2}\Delta\omega^{1/2}\ \gamma\ H_1\ T_1^{1/2}$ is bigger by a factor of $3^{1/2}$. The experimental data easily allow one to distinguish which signal dominates in the high-power limit: they differ by their power dependence. Moreover, as in the example shown in Fig. 2 for perpendicular orientation of the applied field, the sign of the PS is opposite to that of the AS (see icons in Fig. 2).

An example of the detailed fitting procedure is shown in Fig. 1. The shapes of all spectra measured at different micro-

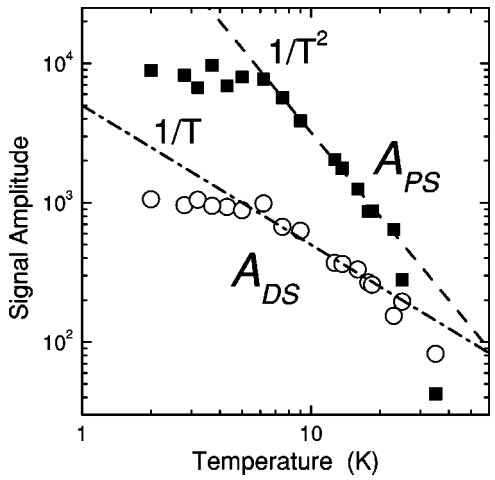

FIG. 3. Temperature dependence of the amplitudes of DS (open circle) and PS (solid squares). The constant amplitudes at low temperature reflect the Pauli susceptibility. The dependences at higher temperatures, where the susceptibility is ruled by the Curie law, show that the DS is proportional to the spin polarization η_0 and for the PS to η_0^2.

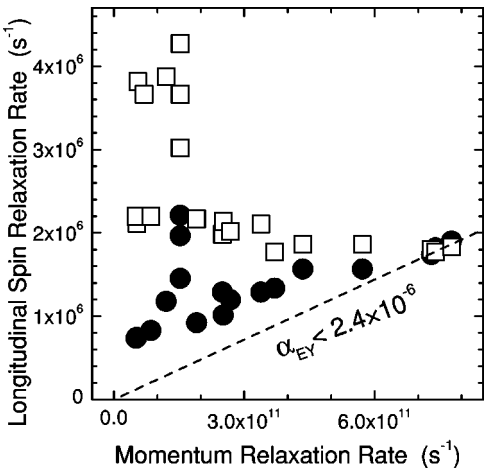

FIG. 4. The longitudinal relaxation rate $1/T_1$ (solid dots) and the double linewidth $2\Delta\omega = 1/T_1 + 2/T_2$ (open squares) measured at $\theta_H = 0°$ as a function of momentum relaxation rate. The dashed line stands for the upper limit of the EY rate: $\alpha_{EY} = 2.4\times10^{-6}$.

wave power were fitted simultaneously. The amplitudes of different signals were treated as fitting parameters for each spectrum but a common value of $\Delta\omega$ has been assumed. The value of the parameter p, directly related to T_1, was evaluated directly for spectra measured at high microwave power, where line broadening is visible. To fit signal shapes at low power a quadratic dependence of p on H_1 was assumed. All spectra can be satisfactory described by the discussed set of common parameters. Amplitudes of contributing signals are power independent for a wide range of power. We relate the decrease of A_{PS} at high power to electron heating and high sensitivity of A_{PS} to temperature.

E. Temperature dependence of ESR

The ESR does not depend critically on temperature. The temperature dependence of the linewidth is presented elsewhere.[6] Some line narrowing with increasing temperature is caused by an increasing efficiency of motional narrowing. Also T_1 depends rather weakly on temperature, at least in the temperature range $T<30$ K, where T_1 can be evaluated.

The temperature dependence of the amplitude of the ESR signals is plotted in Fig. 3. The amplitude of the DS shows similar behavior as the AS. Both are proportional to the spin polarization of the 2D electron gas. They are weakly temperature dependent at very low temperature, corresponding to the Pauli susceptibility. At higher temperatures, they decrease with T^{-1}, reflecting Curie-like magnetism that appears when the temperature exceeds the Fermi temperature. This behavior confirms that the AS corresponds to the classical ESR absorption; it is proportional to the imaginary part and the DS to the real part of the magnetic susceptibility.

The amplitude of the PS decreases with T^{-2} in the high-temperature range. This confirms the origin of the PS which is expected to be proportional to the square of spin polarization at thermal equilibrium [see Eq. (10)]—i.e., to the square of the static susceptibility.

We relate the sharp decrease of the signals at $T \geqslant 30$ K to thermal excitation of electrons to states outside the quantum well. At very high microwave power, when $H_1 \geqslant 0.1$ G, the 2D electron gas is effectively heated by the electric absorption. This is evidenced by an additional reduction of the amplitudes of all ESR signals. Comparing the decrease of the signal amplitude under microwave power with the decrease caused by increasing temperature at low power allows us to estimate the real temperature of the electron gas. For the data presented in Fig. 3 the observed amplitude at $P=200$ mW at $T=4$ K is by a factor of 25 smaller than the amplitude expected under the assumption of constant amplitudes in Eq. (11). Such a reduction of the PS amplitude by a factor of 25 corresponds to a temperature of the electron gas of $T=20$ K.

In conclusion, the amplitudes of all three signal components are more sensitive to temperature and to the microwave heating than can be explained in terms of relaxation times which are almost temperature independent. Consequently, the ESR linewidth is less sensitive when applying high microwave power as it is needed for the evaluation of T_1. Because of that, the broadening of the linewidth is more suitable as compared to the saturation of signal amplitude if the evaluation of T_1 is considered.

F. Spin and momentum relaxation rates

In Fig. 4, $1/T_1$ and $2\Delta\omega$ for perpendicular orientation of the applied field are plotted as a function of the momentum relaxation rate τ_k^{-1}. For low-mobility samples the two dependences merge, $2\Delta\omega \cong 1/T_1$, indicating that the longitudinal relaxation is the dominant broadening process. The increase of the spin relaxation rate with increasing momentum scattering rate may indicate the Elliott-Yafet mechanism where the spin-flip probability is predicted to be proportional to the momentum relaxation rate:[2]

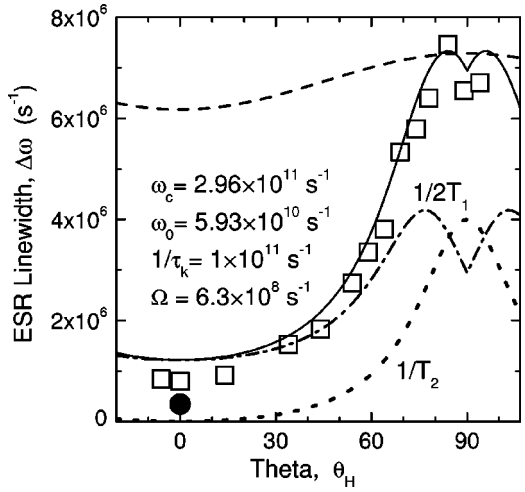

FIG. 5. Angular dependence of the ESR linewidth (squares) at high mobility. θ_H is the angle between the growth direction and the direction of the applied field. The solid dot shows the contribution of the longitudinal relaxation to the linewidth. Dashed line: the anisotropy predicted by Eqs. (13) and (14). The solid, dash-dotted, and dotted lines correspond to Eqs. (4), (26), and (29) for the set of parameters listed in the figure.

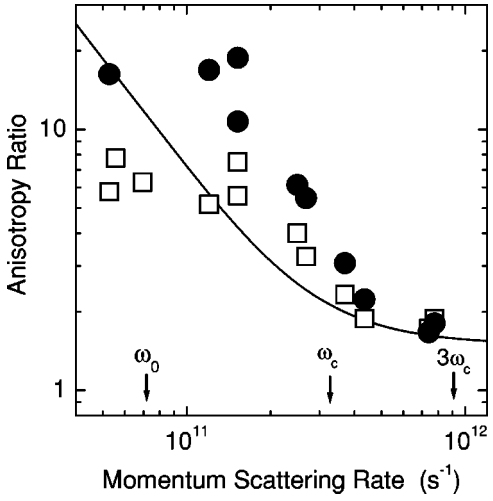

FIG. 6. Anisotropy of the spin relaxation rate as a function the momentum relaxation rate. Open squares: the ratio of the linewidth for in-plane orientation of the applied field, $\Delta\omega(90°)$, and linewidth for perpendicular orientation, $\Delta\omega(0°)$. Solid circles: ratio of $\Delta\omega(90°)$ and the longitudinal contribution to the linewidth, $1/2T_1(0°)$. The solid line shows the anisotropy predicted by Ω_{BR} as described by Eqs. (4), (26), and (29).

$$\frac{1}{T_1} = \alpha_{EY}\frac{1}{\tau_k}. \tag{12}$$

Here the EY coefficient α_{EY} depends on the amount of admixture of different spin states and reflects the probability that a spin-flip process occurs in a momentum scattering event. The data in Fig. 4 allow one to estimate an upper limit for the EY coefficient: $\alpha_{EY} \leqslant 2.4\times 10^{-7}$.

For high electron mobility (low τ_k^{-1}) both $2\Delta\omega$ and $1/T_1$ are much bigger than estimated by the upper limit of the EY spin relaxation rate. This shows that another spin relaxation mechanism becomes dominant in this mobility range. We will argue below that there the longitudinal relaxation is caused by the DP relaxation.

G. Anisotropy of the ESR linewidth

Tilting the applied magnetic field away from the perpendicular direction ($\theta_H \neq 0$), the resonance linewidth increases strongly (see Fig. 5). For high-mobility samples the linewidth increases almost by one order of magnitude. For low-mobility samples, the angular dependence of the linewidth is close to a ($\sin^2\theta_H$) dependence,[6] but for high mobility the dependence is relatively weaker for small θ_H and shows a maximum for $\theta_H \cong 80°$.

The in-plane ($\theta_H = 90°$) linewidth is isotropic for all mobility values, independent of the in-plane direction of the applied magnetic field.

The spin relaxation anisotropy is a clearly pronounced but unexpected experimental finding. None of the known models of spin relaxation predicts such a strong anisotropy. In a previous paper we showed that the transverse DP spin relaxation caused by the BR field, which dominates the spin relaxation for-in plane orientation of magnetic field, is highly anisotropic and vanishes for perpendicular orientation of the magnetic field:[6]

$$\frac{1}{T_2} = \Omega^2\frac{\sin^2\theta_H}{2}\tau_k. \tag{13}$$

The same model predicts also an anisotropy for the longitudinal spin relaxation rate, which is then described by

$$\frac{1}{T_1} = \Omega^2(1+\cos^2\theta_H)\frac{\tau_k}{1+\omega_0^2\tau_k^2}. \tag{14}$$

Here Ω^2 is the variance of the distribution in resonance frequency, caused by a distribution of in-plane oriented SO fields, and ω_0 is the Larmor frequency. For small $\omega_0\tau_k$, the total linewidth [see Eq. (4)] is expected to be isotropic. For sizable $\omega_0\tau_k$, we expect the anisotropy caused by the factor $1/(1+\omega_0^2\tau_k^2)$ as given by the dashed curve in Fig. 5. Obviously this effect is much too small to explain the observed anisotropy.

An anisotropy of the linewidth occurs for all Si/SiGe samples investigated. As is shown in Fig. 6, the anisotropy increases with increasing momentum relaxation time. The ratio of the linewidth for in-plane and perpendicular orientations (open squares in Fig. 6) varies from 8 for a high-mobility sample to 1.7 for low-mobility samples. The anisotropy defined as the ratio of the linewidth for in-plane field for half the longitudinal relaxation rate for perpendicular for high-mobility samples is even more pronounced.

To investigate this effect we follow the ratio of the in-plane linewidth and the longitudinal spin relaxation for perpendicular orientation of the magnetic field where the transverse DP relaxation is expected to vanish. If the origin of both is the same, that ratio should be independent of the

magnitude of the SO field. Moreover, this way we bypass the problem of any additional inhomogeneous broadening which is comparable to the longitudinal relaxation for ($\theta_H = 90°$) but can be easily neglected as compared to the linewidth for ($\theta_H = 90°$). The ratio of the ESR linewidth for ($\theta_H = 0°$) and half the longitudinal spin relaxation rate for ($\theta_H = 90°$) is plotted in Fig. 6 by solid dots as a function of τ_k^{-1}. To estimate the possible errors, the open squares are given: they stand for the ratio of the linewidth for the two orientations.

In our experiment, we are not able to properly evaluate the longitudinal relaxation rate for arbitrary directions of the magnetic field since then there is an in-plane component of the microwave electric field in some parts of the sample. In that case the microwaves are strongly perturbed by the sample and we are not able to estimate the real microwave field amplitude H_1 anymore.

III. MODEL OF SPIN RELAXATION

The observed dependence of the spin relaxation on the momentum scattering rate cannot be explained by any known mechanism. In the discussion below we argue that the peculiarities are caused by the high electron mobility and the resulting cyclotron motion which causes an additional modulation of the effective field seen by the electrons. The discussion begins with a definition of the effective field for different types of zero-field spin splitting. Then the model of spin relaxation at moderate magnetic field, $\omega_c \tau_k \simeq 1$, caused by the modulation of the effective SO field—i.e., the DP spin relaxation—is presented. Finally, the experimental results are discussed.

A. Zero-field spin splitting

The D'yakonov-Perel[3] mechanism for spin relaxation originates from the **k**-dependent spin splitting of the electronic band states. Such zero-field splitting can occur in structures lacking inversion symmetry. The linear antisymmetric term is known as the BR term and has the form of the vector product[9]

$$\mathcal{H}_{BR} = \alpha_{BR}(\sigma \times \mathbf{k}) \cdot \mathbf{n}. \tag{15}$$

Here σ_α are Pauli matrices and the vector **n** is parallel to the symmetry axis (the growth direction for 2D layers). The BR spin splitting can originate from BIA due to an axial symmetry of the crystal[8] or it can result from a SIA due to lack of the mirror symmetry of the quantum well.[9]

A higher-order antisymmetric term, which leads to zero-field spin splitting, has been introduced by Dresselhaus.[10] In cubic crystals lacking inversion symmetry, the DS term has the form

$$\mathcal{H}_{DS} = \gamma_{DS}[\sigma_x k_x (k_y^2 - k_z^2) + \sigma_y k_y (k_z^2 - k_x^2) + \sigma_z k_z (k_x^2 - k_y^2)]. \tag{16}$$

Here γ_{DS} is a material parameter. The DS spin splitting is the dominant effect in crystals, e.g., of zinc-blende structure.

In 2D structures, when the growth direction is parallel to the cubic axis ($\hat{z}$), the mean value $\langle k_z \rangle = 0$ and the DS term has the form

$$\mathcal{H}_{DS} = \gamma_{DS}[\sigma_x k_x (k_y^2 - \langle k_z^2 \rangle) + \sigma_y k_y (\langle k_z^2 \rangle - k_x^2)]. \tag{17}$$

The mean value $\langle k_z^2 \rangle$ does not vanish but it depends on the width of the quantum well and on the number of occupied electric subbands. In that sense it is an independent material parameter. The formation of a 2D structure, however, can modify the value of γ_{DS}. Moreover, γ_{DS}, which vanishes due to high symmetry in bulk Si, does not vanish in Si 2D structures anymore. Consequently, the possibility of such a high-order SIA spin splitting should be considered also in 2D Si structures. According to theoretical calculations the magnitudes of the BR and structure-induced DS splitting are of the same order of magnitude.[16,17]

For the evaluation of the experimental data we consider both types of zero-field spin splittings as described by Eqs. (15) and (17). Consequently, we introduce a set of three different material parameters α_{BR}, γ_{DS}, and $\langle k_z^2 \rangle$ or, equivalently, a set of three independent magnitudes of the zero-field splitting:

$$\hbar \Omega_{BR} = \alpha_{BR} k, \tag{18}$$

$$\hbar \Omega_{DS1} = \gamma_{DS}\left(\langle k_z^2 \rangle k - \frac{k^3}{4} \right), \tag{19}$$

$$\hbar \Omega_{DS3} = \gamma_{DS} \frac{3k^3}{4}. \tag{20}$$

The first stands for BR splitting; the two other terms originate from DS splitting. DS1 varies linearly with **k** vector while DS3 is proportional to k^3.

When the in-plane direction of the **k** vector of an electron is φ_k around the crystal axis then each of the three independent terms resulting from Eqs. (15) and (17) can be described in the form of a scalar product $\mathcal{H} = \hbar \mathbf{\Omega} \cdot \boldsymbol{\sigma}$, where the vectors

$$\mathbf{\Omega}_{BR} = \Omega_{BR}[-\sin\varphi_k, \cos\varphi_k, 0], \tag{21}$$

$$\mathbf{\Omega}_{DS1} = \Omega_{DS1}[-\cos\varphi_k, \sin\varphi_k, 0], \tag{22}$$

$$\mathbf{\Omega}_{DS3} = \Omega_{DS3}[-\cos 3\varphi_k, -\sin 3\varphi_k, 0] \tag{23}$$

are equivalent to vectors of effective SO fields acting on the electron spin, $\mathbf{H}_{SO} = \mathbf{\Omega}/\gamma$.

All effective fields are oriented in plane. Each of them has a uniform in-plane distribution. As a consequence, if one of the fields occurs, then the resulting phenomena are characterized by axial symmetry. Then all directions of the **k** vector, φ_k, and all directions of the in-plane applied field, φ_H, are equivalent.

When the different components of the SO field are of similar amplitude then an in-plane anisotropy can be expected.[18] The fields Ω_{BR} and Ω_{DS1} are similar. They differ by their phase due to the dependence on φ_k only. Because of that, they are hardly distinguishable by experiment. The field caused by Ω_{DS3} is characterized by a 3 times faster dependence on φ_k. As a consequence the momentum scattering or the cyclotron motion causes much faster modulation of this component.

B. D'yakonov-Perel spin relaxation

1. Classical DP relaxation in a 2D electron gas

The effective field acting on an electron affects its resonance frequency, while a time-dependent perturbation results in a finite probability for a spin flip; i.e., it leads to longitudinal spin relaxation. Simultaneously, the spread of the effective fields, originating from the distribution of **k** vectors, leads to a spread in resonance frequencies—i.e., to a broadening of the resonance line. In that sense it contributes to the decoherence of spin precession and thus to transverse spin relaxation.

According to general rules[19] the spin relaxation rate corresponds to the Fourier transforms (FT's) of the time-dependent components of the perturbing fields or, strictly speaking, to the FT's of the autocorrelation function of the effective field. The expressions of Eqs. (13) and (14) correspond to the autocorrelation function of a simple exponential decay, $\Omega^2\exp(-\tau/\tau_k)$, resulting from momentum scattering. The decoherence rate $1/T_2$ corresponds to the zero-frequency component of the autocorrelation function for fluctuations parallel to the applied magnetic field. The longitudinal rate $1/T_1$ is obtained as the FT's of the autocorrelation function for the perpendicular components of the effective field at the Larmor frequency ω_0. The different Fourier components result in different dependences of the relaxation rates on τ_k.

The differences in the angular dependences reflect the planar distribution of the SO fields. The decoherence rate $1/T_2$ is ruled by the fluctuation of SO fields parallel to the external field while a spin flip is caused by the fluctuation of the transverse component of SO field.

2. DP spin relaxation under an external magnetic field

In the case of a strong magnetic field the electron **k** vector changes not only due to momentum scattering but also due to the cyclotron motion. Consequently, the effective modulation frequency of the SO field is bigger, leading to a more effective motional narrowing of the linewidth and to a reduction of the longitudinal spin relaxation.

The direction of the **k** vector rotates in time, $\varphi_k(t)=\omega_c t$, with the cyclotron frequency ω_c. The resulting autocorrelation function of the **k** vector is then $\langle\mathbf{k}(\tau)\mathbf{k}\rangle=k^2\langle\cos\varphi_k(\tau)\rangle=k^2\exp(i\omega_c t-\tau/\tau_k)$. The strengths of the effective fields, as described by Eqs. (21)–(23), are invariant but their directions change in time. $\mathbf{\Omega}_{BR}$ rotates in plane with frequency ω_c. The autocorrelation function of the BR field is then

$$\langle\mathbf{\Omega}_{BR}(\tau),\mathbf{\Omega}_{BR}\rangle=\Omega_{BR}^2\exp(i\omega_c t-\tau/\tau_k). \tag{24}$$

$\mathbf{\Omega}_{DS1}$ rotates in the opposite direction with the frequency $-\omega_c$, while the field $\mathbf{\Omega}_{DS3}$ rotates at a 3 times higher frequency $-3\omega_c$, and the resulting autocorrelation function is

$$\langle\mathbf{\Omega}_{DS3}(\tau),\mathbf{\Omega}_{DS3R}\rangle=\Omega_{DS3}^2\exp(-3i\omega_c t-\tau/\tau_k'). \tag{25}$$

Here the prime at the momentum relaxation times indicates that in that case the relaxation time is obtained by averaging $3\varphi_k$. For a small-angle scattering process, τ_k' is expected to be shorter as compared to τ_k.[11]

The expressions for the spin relaxation rates, caused by the different types of zero-field splitting, are not equivalent anymore. The expressions for the longitudinal relaxation are

$$\frac{1}{T_1}=\Omega_{BR}^2(1+\cos^2\theta_H)\frac{\tau_k}{1+(\omega_0-\omega_c)^2\tau_k^2}, \tag{26}$$

$$\frac{1}{T_1}=\Omega_{DS1}^2(1+\cos^2\theta_H)\frac{\tau_k}{1+(\omega_0+\omega_c)^2\tau_k^2}, \tag{27}$$

$$\frac{1}{T_1}=\Omega_{DS3}^2(1+\cos^2\theta_H)\frac{\tau_k'}{1+(\omega_0-3\omega_c)^2\tau_k'^2}. \tag{28}$$

Here $\Omega^2(1+\cos^2\theta_H)$ is the variance of the SO field perpendicular to the applied field. The transverse relaxation rate is ruled by the variance of the longitudinal component of the SO field, $\Omega^2\sin^2\theta_H$. They are given by

$$\frac{1}{T_2}=\Omega_{BR}^2\frac{\sin^2\theta_H}{2}\frac{\tau_k}{1+\omega_c^2\tau_k^2}, \tag{29}$$

$$\frac{1}{T_2}=\Omega_{DS1}^2\frac{\sin^2\theta_H}{2}\frac{\tau_k}{1+\omega_c^2\tau_k^2}, \tag{30}$$

$$\frac{1}{T_2}=\Omega_{DS3}^2\frac{\sin^2\theta_H}{2}\frac{\tau_k'}{1+9\omega_c^2\tau_k'^2}. \tag{31}$$

These formulas differ in details but generally they contain a reduction factor of the order $(\omega_c\tau_k)^2$ when the relaxation is caused by BR or DS1 and by a bigger factor $9(\omega_c\tau_k')^2$ when caused by DS3. This difference in the dependence of the spin relaxation rate on τ_k allows us to evaluate the dominant type of SO field when the dependence of the spin relaxation on τ_k is analyzed.

These expressions were found under the assumption that the SO field, momentum scattering, and cyclotron motion are weak perturbations of a free-electron state, with a well-defined momentum **k**. From that point of view, the model presented should not be applied for the case when Landau quantization is well pronounced. On the other hand, the obtained expression reflects well the trends expected for the case of strong quantization.[9,21] They show the effect of the suppression of spin relaxations and the scaling of the spin relaxation rates with the square of the SO coupling. For the limit $\omega_0\tau_k\gg1$, the expressions (26)–(31) predict proportionality of the spin relaxation rates to the momentum relaxation rate where the proportionality coefficient is given by the square of the ratio of SO and cyclotron splitting. Such a dependence is also expected when we discuss the probability of a spin flip which accompanies the transition between discrete states. These reasons can explain why the discussed model reasonably fits the experimental data also outside the range of the initial assumptions. The agreement, however, should be treated rather as qualitative than quantitative.

IV. DISCUSSION OF THE EXPERIMENTAL DATA

A. Suppression of DP relaxation by cyclotron motion

For low mobility, when $\omega_c \tau_k \ll 1$, the expressions for spin relaxation caused by the different kinds of SO splitting become equivalent and tend to the classical formulas, Eqs. (13) and (14). For high mobility, however, when $\omega_c \tau_k > 1$, all DP relaxation rates described by formulas (26)–(31) are expected to be suppressed by the cyclotron motion. The suppression is well visible in the experiment. The observed spin relaxation rate for perpendicular orientation is by an order of magnitude smaller than for in-plane orientation, where $\omega_c = 0$, or in comparison to the relaxation rates estimated by Eqs. (13) and (14) when the modulation of the SO field by cyclotron motion is neglected and Ω is taken from other experimental data.[6]

Analyzing the angular dependence of the spin relaxation brings more direct evidence of the effect of cyclotron motion. Generally, the dependence of the relaxation rates on the direction of the applied magnetic field, θ_H, comes from the angular dependence of the variance of the longitudinal and transverse components of SO field [see Eqs. (26)–(31)] and of the cyclotron frequency of 2D electrons, $\omega_c = \omega_{c0} \cos \theta_H$. The former origin causes a strong anisotropy of both contributions $1/2T_1$ and of $1/T_2$ but it does not lead to any strong anisotropy of the total linewidth $\Delta\omega$ (see the dotted line in Fig. 5). In that sense, the anisotropy of the linewidth observed is a fingerprint of the suppression of the spin relaxation by the cyclotron motion.

Moreover, according to Eqs. (26)–(31), the anisotropy ratio, as plotted in Fig. 6, does not depend on the magnitude of the zero-field splitting but on the anisotropy of the modulation rates, caused predominantly by the anisotropy of the 2D cyclotron frequency.

B. Dominance of the BR contribution

When different types of SO splitting [Eqs. (18)–(20)] occur simultaneously then the total relaxation rate is obtained not only by the simple sum of expressions (26)–(31) but also some additional terms caused by interference effects have to be considered. For example the interference of the two linear terms in the absence of an external magnetic field has been discussed by Averkiev *et al.*[18] They showed that in the case when Ω_{BR} and Ω_{DS1} are of similar order of magnitude the expression for the total spin relaxation is more complex. The spin relaxation rate becomes anisotropic and dependent on the in-plane direction φ_H.

The fact that the observed linewidth for in-plane orientation of the magnetic field does not depend on the in-plane direction of the applied field, φ_H, implies that the interference effects of Ω_{BR} and Ω_{DS} are weak and, consequently, that the spin relaxation is dominated by one of the discussed types of SO splitting defined by Eqs. (18)–(20).

Some conclusion can be drawn from the type of angular dependence of the linewidth. The differences in the denominators in the Eqs. (26)–(28), describing the longitudinal spin relaxation rates, shows that the observed maximum of the linewidth, which occurs for $\theta_H < 90°$ (see Fig. 5), corresponds to the minimum of the denominator. Because in Si both frequencies ω_c and ω_0 are of the same sign, the observed maximum of $\Delta\omega$ indicates that the contribution can be caused by Ω_{BR} or Ω_{DS3} but not from Ω_{DS1}. Moreover, keeping in mind that only one of the discussed SO contributions is dominant, we can conclude that the effect of Ω_{DS1} is really negligible.

To conclude whether Ω_{BR} or Ω_{DS} dominates we rely on a quantitative evaluation of the angular dependence or on the estimation of the parameters as described by Eqs. (18)–(20). The lines in Fig. 5 were calculated under the assumption that the BR term is the only contribution. The momentum relaxation rate was found from the cyclotron resonance linewidth. The frequencies ω_0 and ω_c are precisely known from the experiment. Thus Ω_{BR} is a single fitting parameter. The reasonable fit indicates BR as the dominant type of SO coupling. Also the solid line in Fig. 6 is plotted under the assumption that BR is the only SO contribution. The anisotropy of the linewidth caused by the Ω_{DS3} contribution is expected to be much more pronounced.

The angular dependence of $\Delta\omega(\theta_H)$ shows that in the investigated Si layers the linear DS term Ω_{DS1} can be neglected. Since both amplitudes Ω_{DS1} and Ω_{DS3} have the same origin, one can show that in the investigated structures also Ω_{DS3} can be neglected. The width of the quantum well allows us to estimate $\langle k_z^2 \rangle^{1/2} \cong 10^7$ cm^{-1} while the Fermi **k** vector corresponding to an electron concentration of 3×10^{11} cm^{-2} is $k \cong 10^6$ cm^{-1}, an order of magnitude smaller. As a consequence, according to Eqs. (18) and (20), Ω_{DS3} is expected to be by an order of magnitude smaller than Ω_{DS1}. Thus it can be also well neglected.

The value $\Omega_{BR} = 6.3 \times 10^8$ s^{-1} (see data in Fig. 5) corresponds to a BR field of 36 G, and it matches well the BR coefficient as evaluated from *g*-factor and linewidth analysis.[6]

Summarizing, the analysis of experimental data shows that in the investigated Si/SiGe structures the zero-field splitting is dominated by the BR effect. Some deviation between experimental data and the theoretical prediction described by the model can originate from other mechanisms of spin relaxation or from the limited validity of the model which should not be applied for well-pronounced Landau quantization. The observed spin relaxation for perpendicular orientation is, however, extremely slow. It indicates that the spin relaxation rate of other relaxation mechanisms is very small. In the whole investigated range the DP relaxation dominates the total spin relaxation. It stands also for low-mobility samples where the observed anisotropy is well described by a model which considers DP relaxation only. In the case of an important contribution of the EY mechanism a smaller anisotropy would be expected.

V. CONCLUSIONS

Our comparison of the experimental data with the model explains the observed anisotropy quite well. We are not able to estimate the possible fluctuation of the in-plane magnetic field, caused by fluctuations of the perpendicular component of the electric field as postulated by Sherman.[20] Such fluc-

tuations are expected to be characterized by a fast dependence on the electron position. The characteristic length is of the order of a few nm, so the corresponding modulation frequency, seen by an electron moving with the Fermi velocity (3×10^6 cm/s), is very high (10^{12} s^{-1}) and leads to very small spin relaxation.

The expressions for spin relaxation [Eq. (28)–(31)) which take into account modulation of the SO fields by the cyclotron motion indicate the following.

(i) Spin relaxation can be strongly reduced by the applied field.

(ii) The effect becomes important for high electron mobility, when $\omega_c\tau_k \geqslant 1$.

(iii) For increasing $\omega_c\tau_k$ both components of spin relaxation decrease. It reflects the known fact that for $\omega_c\tau_k \gg 1$, when Landau quantization occurs, new eigenstates are formed.[21]

We estimate the upper limit of the EY spin relaxation rate but our data do not prove the occurrence of effective EY relaxation. Just opposite, the strong anisotropy of spin relaxation observed in the whole range of the momentum scattering rate indicates that the DP relaxation is the dominant mechanism of spin relaxation.

Electron-electron scattering may involve the exchange of the magnetic moments among the two electrons. Such an event does not change, however, the total magnetic moment. In that sense, it does not affect the longitudinal relaxation rate. But it causes decoherence—i.e., dephasing (in spite of the fact that the total magnetic moment, including the transverse component, is invariant).

The effect of damping of the spin relaxation by the cyclotron motion is expected to be much more efficient for the cubic DS term. Because of that, it is expected to be of great importance in III-V semiconductors where the DS splitting is by orders of magnitude bigger. But the spin relaxation can be effectively reduced by the external field. The observed linewidth of spin resonance in high-mobility GaAs at high magnetic field is very narrow, indicating the suppression of DP relaxation by the cyclotron motion.

The effect of the suppression of the spin relaxation by can be applied in spintronic devices where a long spin memory is needed.[4,5]

ACKNOWLEDGMENTS

We thank F. Schäffler (JKU) for generously providing samples and helpful discussions. We also appreciate very stimulating and helpful discussions with P. Vogl, J. Majewski, and E. Sherman. This work was supported by KBN Grant No. PBZ 044/P03/2001 and 2 P03B 054 23 in Poland and in Austria by the Fonds zur Förderung der Wissenschaftlichen Forschung, and ÖAD, both Vienna.

*Electronic address: wilamz@ifpan.edu.pl

[1] Y. Yafet, in *Solid State Physics*, edited by F. Seitz and D. Turnbull (Academic Press, New York, 1963), Vol. 14, p. 1.
[2] R.J. Elliott, Phys. Rev. **96**, 266 (1954); Yafet (Ref. 1).
[3] M.I. D'yakonov and V.I. Perel', Sov. Phys. JETP **38**, 177 (1973).
[4] S. Datta and B. Das, Appl. Phys. Lett. **56**, 665 (1990).
[5] H. Jaffer and A. Fert, J. Appl. Phys. **91**, 8111 (2002).
[6] Z. Wilamowski, W. Jantsch, H. Malissa, and U. Rössler, Phys. Rev. B **66**, 195315 (2002).
[7] Z. Wilamowski, W. Jantsch, N. Sandersfeld, M. Mühlberger, F. Schäffler, and S. Lyon, Physica E (Amsterdam) **16**, 111 (2003).
[8] E.I. Rashba, Fiz. Tverd. Tela (Leningrad) **2**, 1224 (1969) [Sov. Phys. Solid State **2**, 1109 (1960)].
[9] Yu.L. Bychkov and E.I. Rashba, J. Phys. C **17**, 6039 (1984).
[10] G. Dresselhaus, Phys. Rev. **100**, 580 (1955).
[11] F.G. Pikus and G.E. Pikus, Phys. Rev. B **51**, 16 928 (1995).
[12] A.M. Tyryshkin, S.A. Lyon, W. Jantsch, and F. Schäffler (unpublished).
[13] Z. Wilamowski, N. Sandersfeld, W. Jantsch, D. Többen, and F. Schäffler, Phys. Rev. Lett. **87**, 026401 (2001).
[14] Z. Wilamowski and W. Jantsch, Physica E (Amsterdam) **10**, 17 (2001).
[15] C.P. Poole, *Electron Spin Resonance*, 2nd ed (Wiley, New York, 1983).
[16] P. Vogl and J.A. Majewski, in Institute of Physics Conference Series No. 171, edited by A.R. Long and J.H. Davies (Institute of Physics, Bristol, UK, 2003), P3.05, ISBN 7503-0924-5; (private communication).
[17] J.A. Majewski, P. Vogl, and P. Lugli, in Proceedings of the 25th International Conference on the Physics of Semiconductor, Osaka, 2000, edited by N. Miura and T. Ando (Springer, Berlin, 2001), p. 791.
[18] N.S. Averkiev, L.E. Golub, and M. Willander, J. Phys.: Condens. Matter **14**, R271 (2002).
[19] A. Abragam, *The Principles of Nuclear Magnetism* (Clarendon Press, Oxford, 1961).
[20] E.Ya. Sherman, Appl. Phys. Lett. **82**, 209 (2003).
[21] For a review see E.I. Rashba and V.I. Sheka, in *Landau Level Spectroscopy*, edited by G. Landwehr and E.I. Rashba (Elsevier Science, Amsterdam, 1991).